

reasonable fit is obtained for intensity values from 8×10^{12} to 2×10^{13} W cm^{-2} , in good agreement with the experimental value $(8 \pm 2) \times 10^{12}$ W cm^{-2} . One should note that at this intensity, and for the second harmonic, formula (2) gives an energy gain in the gradient of the field of 0.25 eV which is compatible with the experimental width of the peaks of 0.5 eV and which, in any case, leaves the two peaks well resolved.

We are in the process of obtaining additional information regarding the electrons emitted in N -photon ionization. These include the measurement of angular distribution and the dependence on polarization. A comprehensive account will be published elsewhere.

We finally wish to remark that our measure-

ment has been the first to detect an additional photon absorption beyond the minimum number necessary for ionization of an atom.

¹L. A. Lompre, G. Mainfray, C. Manus, and J. Thebault, *Phys. Rev. A* **15**, 1604 (1977).

²T. W. B. Kibble, *Phys. Rev. A* **150**, 1060 (1966).

³E. A. Martin and L. Mandel, *Appl. Opt.* **15**, 2378 (1976).

⁴M. J. Hollis, *Opt. Commun.* **25**, 395 (1978).

⁵E. Karule, *J. Phys. B* **11**, 441 (1978).

⁶N. K. Rahman, *Phys. Rev. A* **10**, 440 (1974).

⁷A. Weingarsthofer, J. K. Holmes, G. Candle, E. Clarke, and H. Kruger, *Phys. Rev. Lett.* **39**, 269 (1977).

Measurement of Differential Cross Sections for the Elastic Scattering of Positrons by Argon Atoms

P. G. Coleman and J. D. McNutt

Department of Physics, The University of Texas at Arlington, Arlington, Texas 76019

(Received 14 December 1978)

Direct measurements of differential scattering cross sections for positron-gas-atom collisions are reported. The apparatus used exploits the time-of-flight technique. Results for positrons of mean energy 2.2, 3.4, 6.7, and 8.7 eV elastically scattered through angles between 20° and 60° by argon atoms are presented. Sources of experimental error are discussed and comparison with recent theoretical calculations is made.

In this Letter directly measured values of differential cross sections for the elastic scattering of positrons by gas atoms are reported. During the past decade the experimental determination of positron-atom total scattering cross sections¹⁻³ has ensued from the discovery that a small fraction (typically 10^{-5} or 10^{-6}) of fast positrons incident upon a solid surface are moderated and reemitted with a narrow spectrum of energies peaked at about 1 eV or less. The time-of-flight (TOF) technique⁴ is particularly suited to differential-cross-section measurements for positrons where, using currently available source/moderator assemblies, the scattered intensity into a detector subtending a small solid angle at the scattering center would be impractically low. Spatial separation is replaced by TOF separation, and intensities over all forward angles can, in principle, be measured simultaneously.

The TOF spectrometer designed for these measurements utilizes a source assembly similar to that described by Coleman *et al.*⁵; fast pos-

itrons from a $30\text{-}\mu\text{Ci } ^{22}\text{Na}$ source pass through a 0.25-mm-thick fast-plastic-scintillator disk, and almost all positrons emerging from the disk have produced a light flash which initiated a fast electrical timing pulse in the photomultiplier tube. The fast positrons then strike a circular 325-gauge (40% transmission) stainless steel grid coated thinly with MgO powder and the slow positrons which emerge, at a rate of about 10 sec^{-1} from the 10-mm-diam grid, possess a mean energy $\bar{E} \approx 1.6 \text{ eV}$ with a spread of about 1.5 eV. The slow positrons are accelerated axially in the 1-mm gap between the coated grid, to which a potential V is applied, and a 325-gauge grounded grid.

The diameter of the positron beam is determined by the 3.5-mm-diam hole in the brass plate which supports the grounded grid. The flux of slow positrons which passes through the hole is reduced to about 0.5 sec^{-1} . The brass plate forms the top of a 10-mm-long gas cell in which the scattering takes place. The slow positrons

leave the cell through a 5.5-mm-diam exit port in a 5-mm-thick plate. They then travel down a 25-cm-long flight path to be collected on the 10-mm-diam cone of a channel electron multiplier (CEM). After being accelerated to 300 eV between two grids located directly above the CEM cone, the slow positrons are detected with almost 100% efficiency⁶ and produce fast timing pulses signaling their arrival. The CEM is insensitive to the 0.51- and 1.28-MeV γ rays emitted from the source region so that a short, straight flight tube could be used and a good signal-to-background ratio achieved. The source support flange is movable to an extent which allows positioning of the source directly above the center of the CEM cone. The photomultiplier and CEM pulses are fed into standard fast-timing electronic units and TOF spectra are accumulated.

The source, gas cell, and CEM are contained in a 15-cm-diam vacuum chamber which is mounted vertically upon a 15-cm oil vapor diffusion pump. A second 15-cm pump is connected to the top of the chamber by a 7.5-cm \times 5.1-cm waveguide section, and oil backstreaming is reduced by water-cooled baffles. A base pressure in the 10^{-7} Torr range is achieved, as measured by an ionization gauge head mounted on the CEM support flange. Upon introducing argon into the gas cell through a micrometering valve so that its density in the cell is suitable for scattering measurements (about 0.05 Torr), a residual pressure of 2×10^{-5} Torr is recorded in the main chamber and there is no measurable variation in this value along the flight path from the CEM to within 2 cm of the gas cell. The CEM operates efficiently in the low- 10^{-5} -Torr range. Thus a pressure differential of over 2000:1 is maintained across the cell exit port, and accordingly over 99% of the scattering occurs within the cell. The positrons are guided from source to CEM by an axial magnetic field, measured to be uniform to within 1% (see Griffith *et al.*⁷), produced by a single solenoid which extends well beyond each end of the flight path. A field strength of 140 G is used so that positrons scattered through almost 90° are restricted to follow a helical path of radius less than 1 mm, even at the highest energies used. Every positron which is scattered in the gas cell into the forward hemisphere is able, therefore, to leave the exit port (whose diameter is 2 mm larger than that of the entrance port) and travel to the CEM.

The angular distribution of positrons scattered in the cell is measured in the following manner.

Firstly, with the system evacuated, a TOF spectrum is accumulated. This spectrum has the form of a narrow, peaked signal distribution above a low-level, almost-flat background component. Gas is then leaked continuously into the cell and a second spectrum is recorded. Typical run times are 60 000 s. System stability is checked by repeating the "vacuum" run after the "gas" run; a settling time of about 10 h is usually allowed before commencing data accumulation after the accelerating potential on the coated grid has been changed (see Ref. 5).

If a slow positron, whose initial direction is assumed to be axial, is scattered through an angle θ at a point which for the purpose of this analysis will be assumed to be the midpoint of the cell, then its flight path length and hence its TOF from that point is increased by the multiplying factor $\sec\theta$. A "tail" is therefore seen on the long-time side of the "gas" spectra which represents the time distribution, and hence the angular distribution, of the scattered positrons. The time distribution of scattered positrons is isolated from that of the unscattered positrons by appropriately attenuating the "vacuum" spectrum and subtracting it from the measured "gas" spectrum, after performing standard background-subtraction and signal-restoration procedures.⁸ The attenuation factor, which is determined by the product of the gas density with the effective cell length, is measured directly by repeating the data collection procedure with a very low magnetic field strength, reducing the numbers of scattered positrons collected by the CEM to a minimum. In addition, the shape of the attenuated "vacuum" spectrum is corrected for the variation of the total cross section over the energy spread of the incident beam. Typical measured TOF spectra, illustrating this procedure, are shown in Fig. 1.

The measured scattered positron TOF histogram $(\Delta N_s/\Delta t)_i$ thus describes the numbers of positrons $(\Delta N_s)_i$ which after scattering possess times of flight between t_i and $t_i + \Delta t$, where i denotes the channel number and Δt the channel time width. Because the total attenuation, and hence the total number of scattered positrons N_s , is measured, absolute values for the differential cross section are obtained if the total scattering cross section $Q_T(E)$ is assumed. The Q_T values for Ar used in the present analysis are the measurements of Coleman *et al.*⁹ which agree well with those of Kauppila, Stein, and Jesion¹ in the elastic scattering region. Recalling that the angular distribution of scattered positrons meas-

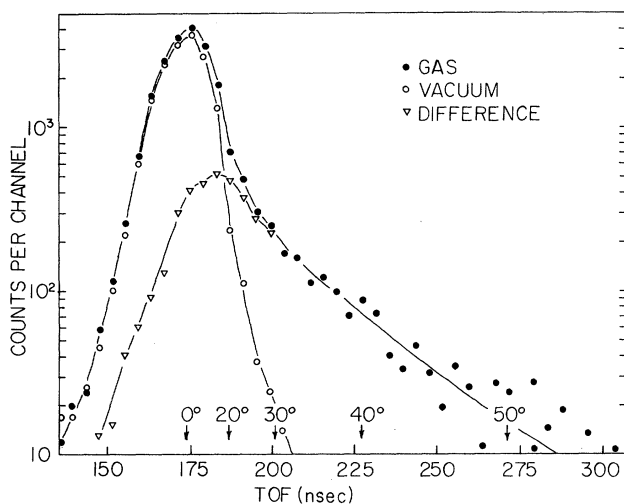


FIG. 1. Multichannel analyzer TOF histograms with and without argon in the gas cell, after signal restoration and background subtraction. Run times 55 000 s, $\bar{E} = 6.7$ eV ($k = 0.7$). Lines drawn through the points are for clarity. The vacuum spectrum is attenuated as described in the text. The difference spectrum is the time distribution of scattered positrons and differs from the gas spectrum only where shown.

ured by this technique is $I \sin \theta$, it is easily shown that the differential cross section I is given by

$$I(\theta_i) = (\Delta N_s / \Delta t)_i (T Q_T \sec^2 \theta_i / 2N_s) a_0^2, \quad (1)$$

where T is the TOF of an unscattered positron of energy \bar{E} , the mean energy of the incident slow positrons, Q_T is the total cross section at \bar{E} in units of πa_0^2 , and θ_i is the angle through which a positron whose TOF is at the center of channel i has been scattered.

Equation (1) strictly applies to the scattering of a truly monoenergetic incident positron beam by a thin planar gas target. In practice, a scattered positron with TOF t_i has been deflected through an angle whose size depends on where in the 1-cm-long gas cell the scattering occurred; i.e., t_i corresponds not to a single θ_i but to a range of angles $\theta_i \pm \Delta \theta_i$ ($\Delta \theta = 2^\circ$ and 0.6° for $\theta = 25^\circ$ and 60° , respectively). The spread in the incident slow positron energies ΔE (full width at half maximum ≈ 1 eV) smears the $\Delta N_s / \Delta t$ distribution so that the measured $I(\theta)$ values, here attributed to positrons of energy \bar{E} , actually are average values over the range ΔE which are strongly weighted near \bar{E} . A first-order correction for the effects of smearing due to the TOF spread of the incident positrons (ΔT) can be made by deconvoluting ($\Delta N_s / \Delta t$) using the incident-positron time distri-

bution as a resolution function; this procedure is based on the approximation that $I(\theta)$ is energy independent over the small interval ΔE , noting in addition that the ratio $\Delta T / T$ is small. Corrections to the measured distribution are significant only below $\theta \approx 25^\circ$ and in the results presented here only two values of $I(\theta)$ are included which have been changed, both by less than 10%, following deconvolution.

As a direct result of the relation between θ_i and t_i , $\Delta N_s / \Delta t$ becomes widely spread in time as θ increases, and it is currently impractical to look for signal above background for scattering angles greater than about 65° .

To summarize, with the present system the best results are obtained for $20^\circ < \theta < 60^\circ$; these results are almost insensitive to small changes in the factor by which the "vacuum" spectrum is attenuated and, in addition, the angles θ_i are well determined.

A fundamental assumption upon which the data analysis is based is the axially of the incident beam direction. When the intrinsic energy of emission of the slow positrons is much smaller than the applied axial accelerating potential V this assumption is straightforwardly justified. Evidence which supports this assumption for low or even zero accelerating potentials is discussed fully by Coleman *et al.*,⁵ who conclude that all their observations support the assumption that the spread in the signal distributions is due to energy dispersion and that very little angular divergence is present.

Argon gas was selected for the first measurements of $I(\theta)$ because its Q_T has been well measured below 8.9 eV,^{1,9} does not vary sharply with energy, and is high enough to allow use of a suitably low cell gas pressure.

The experimental results for $k = 0.4, 0.5, 0.7$, and 0.8 ($\bar{E} = 2.2, 3.4, 6.7$, and 8.7 eV) are presented in Fig. 2. The results of the semiempirical calculation of Schrader¹⁰ and of the polarized orbital calculation of McEachran, Ryman, and Stauffer¹¹ are shown for comparison. The total cross sections of Schrader are in good agreement with those measured by Coleman *et al.*,⁹ whereas those of McEachran, Ryman, and Stauffer are higher. The $I(\theta)$ values of Ref. 11 shown in Fig. 2 have therefore been scaled down by the factor $Q_T(\text{measured}) / Q_T(\text{Ref. 11})$, e.g., 0.70 and 0.87 for $k = 0.4$ and 0.8 , respectively. The shapes of the two calculated $I(\theta)$ curves are seen to be very similar.

It is evident from Fig. 2 that the measurements

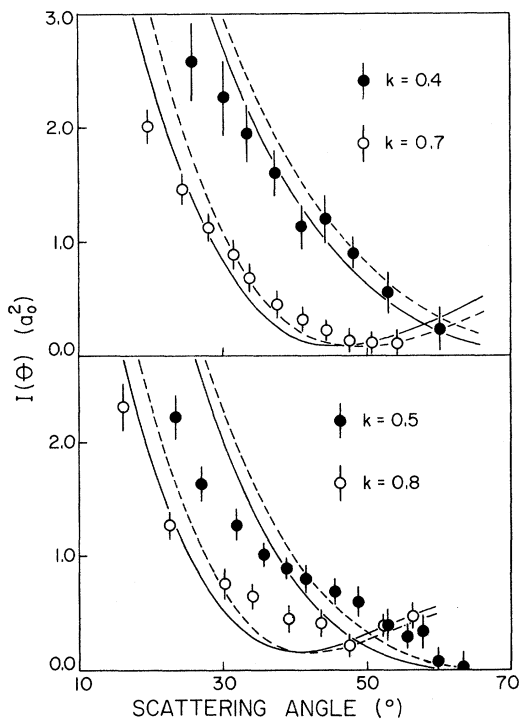


FIG. 2. Experimental results for $I(\theta)$ vs θ at different positron mean energies. The error bars represent statistical standard deviations. Solid lines, calculations of Schrader (Ref. 10); broken lines, scaled-down calculations of McEachran, Ryman, and Stauffer (Ref. 11) (see text).

are in reasonable agreement with the theoretical calculations. A major improvement in the quality of the experimental data will ensue from the development of a narrower incident-positron energy distribution and a greater beam intensity. A smaller energy spread, and hence TOF spread, will make possible measurement at lower angles without the need for resolution corrections. An increase in beam intensity will enable the use of lower scattering-gas densities, decreasing the effects of double or multiple scattering in the cell to an unimportant level. At present the choice of a gas density high enough to produce a scattered signal distribution whose intensity is significant above background has the result that about 20% of the scattered positrons have undergone two collisions in the gas cell. The meas-

ured ratios of the integrated scattered intensity between 0° and 60° to the total scattered intensity (0° – 180°) are generally 10–15% lower than is predicted theoretically,¹⁰ a result which could be explained in terms of double scattering. It should be noted, however, that the values of $I(\theta)$ for θ below 15° are extremely dependent upon the assigned attenuation factor for the “vacuum” spectrum. In conclusion, it is apparent from Fig. 2 that the effects of double scattering, or any other sources of error, are not significant enough to mask the dependence of $I(\theta)$ on positron energy.

The system will be used to measure differential cross sections in other gases over a wider range of positron energies and will in addition be applied to similar measurements for electrons, which are copiously ejected from the MgO powder.

The authors wish to thank Dr. D. M. Schrader and Dr. A. D. Stauffer for communicating their results prior to publication, Dr. L. M. Diana for useful discussions, and J. T. Hutton for helping with construction and data analysis. This work was supported in part by the Robert A. Welch Foundation, Houston, Texas 77002, and by National Science Foundation Grant No. SPI76-83578 A01.

¹W. E. Kauppila, T. S. Stein, and G. Jesion, *Phys. Rev. Lett.* **36**, 580 (1976).

²K. F. Canter, P. G. Coleman, T. C. Griffith, and G. R. Heyland, *J. Phys. B* **5**, L167 (1972).

³J. R. Burciaga, P. G. Coleman, L. M. Diana, and J. D. McNutt, *J. Phys. B* **10**, L569 (1977).

⁴P. G. Coleman, T. C. Griffith, G. R. Heyland, T. L. Killeen, *J. Phys. B* **8**, L454 (1975).

⁵P. G. Coleman, J. D. McNutt, L. M. Diana, and J. R. Burciaga, *Phys. Rev. A* (to be published).

⁶S. Pendyala, J. Wm. McGowan, P. H. R. Orth, and P. W. Zitzewitz, *Rev. Sci. Instrum.* **45**, 1347 (1974).

⁷T. C. Griffith, G. R. Heyland, K. S. Lines, and T. R. Twomey, *J. Phys. B* **11**, (1978).

⁸P. G. Coleman, T. C. Griffith, and G. R. Heyland, *Appl. Phys.* **5**, 223 (1974).

⁹P. G. Coleman, J. D. McNutt, L. M. Diana, and J. T. Hutton, to be published.

¹⁰D. M. Schrader, private communication.

¹¹R. P. McEachran, A. G. Ryman, and A. D. Stauffer, private communication.